Photoinitiated Bulk Polymerization of Liquid Crystalline Thiolene Monomers

Hans T. A. Wilderbeek,*,†,‡ J. (Han) G. P. Goossens,†,‡ Cees W. M. Bastiaansen,*,† and Dirk J. Broer*,†,||

Eindhoven University of Technology, P.O. Box 513, 5600 MB Eindhoven, The Netherlands; Dutch Polymer Institute, P.O. Box 902, 5600 AX Eindhoven, The Netherlands; Philips Research Laboratories, Professor Holstlaan 4, 5656 AA Eindhoven, The Netherlands

Received June 12, 2002; Revised Manuscript Received September 19, 2002

ABSTRACT: The photoinitiated bulk polymerization of liquid crystalline thiolene monomers based on a phenyl benzoate core was investigated and the structure of the corresponding polymers analyzed. We show that polymerization occurs substantially in bulk, and can be initiated on demand by UV-irradiation. The liquid crystalline thiolene polymers exhibit a nematic mesophase, and the molecular weight, molecular weight distribution and overall conversion are characteristic for polymers obtained by a step-growth polymerization. Using NMR spectroscopy, we show that anti-Markovnikov structures are predominantly formed, with a small fraction of the structures displaying different configurations that can be attributed to thiol olefin addition−cooxidation processes or to homopolymerization of the olefinic moiety. The conversions of the thiol and vinyl groups were monitored using time-resolved Raman spectroscopy and dissimilar partial reaction rates were observed.

Introduction

Polymers with a well-defined molecular organization play an important role in applications for information and communication technology.[1] For instance, well-organized conjugated polymers are the basis of polymer light-emitting diodes,[2] oriented polymers are used in polarization optics,[3] and copolymers with well-defined compositional gradients can be found in graded-index polymer optical fibers used for local area network communications.[4]

Liquid crystalline polymers have traditionally also been considered for their distinct anisotropic properties on a molecular scale, and on a macroscopic scale if adequate monolithic alignment can be achieved.[5] Side-chain or network-type based systems are usually employed for optical applications depending on the initial functionality of the monomer. For instance, polymerized monofunctional discotic acrylates are used as compensation foils to improve the viewing angle of liquid crystal displays,[6] whereas bifunctional liquid crystalline acrylates,[7] epoxides,[8] and vinyl ethers[9] are generally used to obtain highly oriented polymer films or to form the basis for various network stabilized liquid crystals effects[10] along with multifunctional thiolenes.[11]

The order parameter associated with the mesogenic moieties in conventional side-chain and network-type systems is comparable to the order parameter of low molar mass liquid crystals, however, and is limited to a maximum of approximately 0.7. Although rotational mobility is hindered, a higher order parameter should in principle be possible, but is limited by the steric hindrance caused by the polymer backbone. This hinders perfect alignment of the mesogenic core, despite the decoupling of the core from the polymer backbone. In the case of *main-chain* liquid crystalline polymers, it is anticipated that the whole molecule will be aligned to a higher degree, resulting from the larger aspect ratio. Consequently, the increased degree of order in main-chain liquid crystalline systems could potentially lead to enhanced optical properties in comparison to side-chain or network-type systems.

Monomers containing mercapto and vinyl groups, i.e. thiolene monomers, can be polymerized via a free-radical propagated step-growth mechanism,[12] leading to the desired main-chain polymers. The synthesis and polymerization of liquid crystalline thiolene monomers has been reported before.[13−15] However, the reported monomers display high transition temperatures originating from their bulky rigid core. A single compound with a smaller mesogenic group based on a double phenyl core was shown to exhibit lower transition temperatures,[13] which is of special importance for obtaining homogeneous mixtures of these monomers with anisotropic solvents, aimed at establishing novel polymer/LC composites. The double phenyl compound therefore served as a template for the synthesis of further liquid crystalline thiolene homologues (Table 1).[16]

In this paper, we describe the photoinitiated bulk polymerization of these liquid crystalline thiolene monomers and the characterization of the corresponding polymers. The in situ polymerization of these thiolene monomers in isotropic and anisotropic media is treated elsewhere.[17]

Theory

The mechanism of photoinitiated thiolene polymerization is schematically shown in Scheme 1.[12] Thiyl radicals RS$^{\bullet}$ can be introduced by a (Norrish) type I[18] or type II[19] initiation (Scheme 1, part II). The initiation reaction is followed by the addition of the thiyl radical to an olefinic moiety, yielding a β-thioether carbon

* Corresponding authors. E-mail: H.T.A.W, hans.wilderbeek@philips.com; C.W.M.B., c.w.m.bastiaansen@tue.nl; D.J.B., dick.broer@philips.com. Present address of H.T.A.W: Philips Research Laboratories, Professor Holstlaan 4, 5656 AA Eindhoven, The Netherlands.
† Eindhoven University of Technology.
‡ Dutch Polymer Institute.
|| Philips Research Laboratories.

10.1021/ma020916l CCC: $22.00
Published on Web 10/26/2002

Scheme 1. Schematic Overview of the Photoinitiated Thiolene Polymerization Mechanism[a]

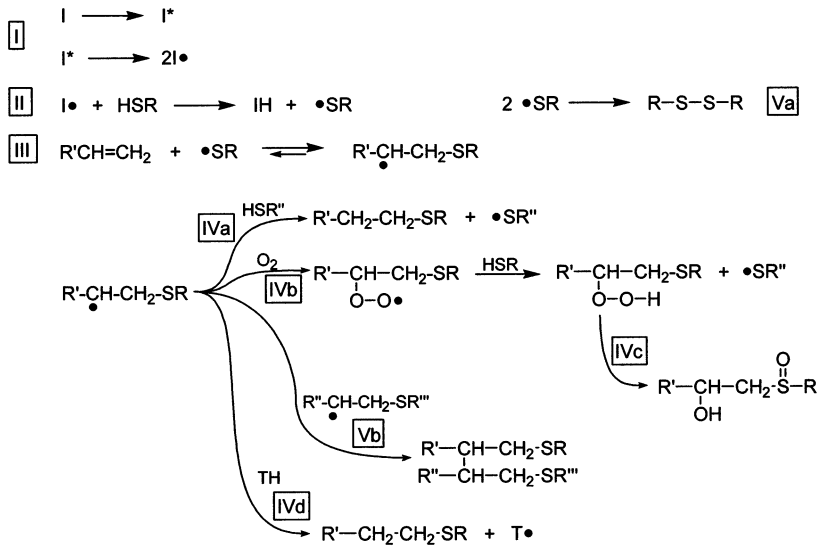

[a] Key: (I) initiator dissociation; (II) initiation; (III) addition reaction; (IVa) propagation; (IVb) cooxidation; (IVc) rearrangement (TOCO); (IVd) transfer; (Va) thiyl radical combination; (Vb) β-carbon radical combination.

Table 1. Structure, Nomenclature, and Transitions (°C) of ThE *mbn* Homologues[16 a]

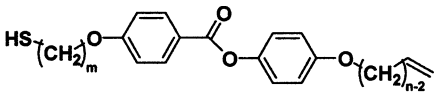

ThE mbn

structure	*m*	*n*	Cr	→	SmA	→	N	→	I
ThE 4b4	4	4		58.6				68.4	
ThE 6b6	6	6		42.5		55.4		69.5	

[a] "Cr" denotes the crystalline phase, "SmA" denotes the smectic A phase, "N" denotes the nematic phase, and "I" denotes the isotropic phase. The indices *m* and *n* refer to the number of carbon atoms in the spacers.

radical (Scheme 1, part III). This step is in principle a reversible reaction, and an equilibrium mixture of a thiyl radical, a β-thioether carbon radical, and an olefin can be obtained.[20] As a result of the slow addition step, the overall reaction rate is best described using a step-growth behavior, despite the free-radical propagation mechanism.

Alternatively, if no free radicals are present to fulfill the role of initiating species, the reaction can proceed by a nucleophilic[12] or electrophilic mechanism. The electrophilic mechanism involves the protonation of the olefin, followed by the addition of the thiol to the carbocation and subsequent deprotonation, obeying Markovnikov's rule.[21] This is in contrast with the free-radical pathway where the thiol olefin addition products show an anti-Markovnikov orientation.

In the free-radical mechanism, the β-thioether carbon radical can follow several pathways. In the absence of oxygen, chain transfer occurs by abstraction of a proton from a thiol, resulting in a regenerated thiyl radical, and thus ensuring the propagation (Scheme 1, part IVa). Alternatively, chain transfer may result in a dormant radical species (Scheme 1, part IVd). Homopolymerization, by addition of the olefin to the carbon radical, is seldom observed, as the reaction rate for homopolymerization is generally lower than the transfer rate to thiol.

A substantial advantage of thiolene polymerizations over conventional free-radical acrylate polymerizations is the insensitivity of the thiolene polymerization process to dissolved or ambient oxygen; in the so-called thiol olefin addition−cooxidation process (TOCO),[22−24] oxygen is incorporated, but the regenerated thiyl radical preserves propagation (Scheme 1, parts IVb and IVc).

Experimental Section

Materials. The liquid crystalline monomers **ThE 4b4** and **ThE 6b6** were synthesized according to previously reported procedures.[16,25] The (Norrish) type I photoinitiator used for the initiation of the polymerizations, Irgacure 651 (α,α-dimethoxydeoxybenzoin), was supplied by Ciba Specialty Chemicals, Basel, Switzerland. Deuterated chloroform-*d* (Merck, Darmstadt, Germany) and deuterated 1,1,2,2-tetrachloroethane-d_2 (Aldrich Chemie, Zwijndrecht, The Netherlands) were used for NMR spectroscopy. HPLC-grade chloroform was used as the eluent for the size exclusion chromatography (SEC), and was supplied by Biosolve, Valkenswaard, The Netherlands. All commercially available materials were used as received.

Characterization Techniques. FT-NMR spectra were recorded using a Varian 400 MHz and an Inova 500 MHz spectrometer at the resonance frequencies of 400.162 and 499.799 MHz, respectively, for ^{1}H-resonance spectra, and 100.630 and 125.686 MHz, respectively, for ^{13}C-resonance spectra. All spectra were recorded in chloroform-*d* or in tetrachloroethane-d_2 at 25 °C. All chemical shifts are reported in ppm relative to the chemical shift of the deuterated solvent ($\delta = 5.93$ ppm for proton and $\delta = 73.76$ ppm for carbon NMR). The coupling constants J are given in hertz. The parameter d_1 was set to 3 s for the polymeric samples.

Thermal characterization was performed using a Perkin-Elmer Pyris 1 differential scanning calorimeter (DSC) equipped with a CCA-7 temperature controller at a heating rate of 10 °C min^{-1}. The DSC was calibrated using indium, zinc, hexatriacontane, *n*-octane, and *n*-dodecane standards of high purity. Texture micrographs were obtained using a Zeiss MC63 microscope with polarization optics in combination with a Linkam THMS 600 hot-stage.

SEC was performed using a Waters type 710B injector (50 μL) and two Polymer Labs, mixed-*d*, 7.8 × 300 mm columns thermostated using a Spark Holland Mistral thermostat at 30 °C. A Waters type 6000 pump provided a constant flow of 1 mL of chloroform min^{-1}. A Waters model 440 UV-detector ($\lambda = 254$ nm and $\lambda = 263$ nm) was used for detection.

Time-resolved Raman spectroscopy was performed using a Dilor Labram spectrometer, equipped with a Peltier air-cooled CCD array detector and a Spectra-Physics laser with an

excitation line of 532 nm. Samples were prepared in sealed capillaries and thermostated using a Linkam THMS 600 hot-stage. Irradiation of the samples was performed using a medium-pressure mercury UV-light source (Oriel Instruments) in combination with a band-pass filter ($\lambda = 365$ nm, half-width 8 nm, effective light intensity at sample position 7 mW cm^{-2} at 365 nm). The acquisition time of each spectrum was 2 s at the initial stage (no time delay between the recording of the sequences) and 10 s at a later stage of the polymerization (increasing the delay from 20 to 110 s in three steps), after the phase separation occurred, to improve the signal-to-noise ratio. The measured intensities were afterward normalized, based on a uniform acquisition time for all sequences. Data analysis involved a polynomial baseline correction and filtering of the raw data using a Savitsky−Golay filtering routine. The nature of the peak shapes did not allow for a simple peak fitting procedure. A combined Gaussian and Lorentzian peak fitting routine was therefore used, with both in-house developed software routines (Matlab library) and commercial software peak-fitting routines (GRAMS/32AI 6.00, Galactic Industries Co.). The analysis was even further complicated in the vinyl band region, where several peaks overlap. Despite correction of the curved baseline, reduction of the noise by filtering, and the use of combined peak fitting routines, a certain degree of scattering in the data remains.

Polymer Synthesis. Photoinitiated polymerizations were carried out in small 30 or 50 μL aluminum DSC sample pans. The quantities, typically 0.5−1.5 mg, were sufficiently small to ensure the formation of a small film of equal thickness in each case. The samples were irradiated using a medium-pressure mercury Philips PL-S 10 UV-light source, connected to a timer at an approximate sample-light source distance of 10 cm (light intensity at sample position 2.7−3.5 mW cm^{-2} at 365 nm). All irradiations were carried out in an inert argon environment, except for the conversion measurements. In all cases, the photoinitiator (Irgacure 651) content was 1% w/w, based on the monomer, unless stated otherwise.

NMR signal assignment for **poly(ThE 4b4)**: ^{13}C NMR ($CDCl_2CDCl_2$; 25 °C; 100.614 MHz): 165.2 ($C^{l'}$), 163.2 ($C^{h'}$), 156.4 ($C^{p'}$), 144.1 ($C^{m'}$), 132.1 ($C^{j'}$), 122.5 ($C^{n'}$), 121.4 ($C^{k'}$), 115.0 ($C^{o'}$), 114.2 ($C^{i'}$), 67.74 + 67.66 ($C^{g'}$ + $C^{q'}$), 31.7 + 31.6 ($C^{b'}$ + $C^{v'}$), 28.3 + 28.1 ($C^{f'}$ + $C^{t'}$), 26.0 + 25.9 ($C^{c'}$ + $C^{u'}$). See the analysis of the corresponding monomer for the carbon assignment of the nonaliphatic region.[16] For the carbon assignment of the aliphatic region, see Scheme 2. The signal assignment of **poly(ThE 6b6)** corresponds with the expected structure and differs only slightly from that of **poly(ThE 4b4)** in the aliphatic region.

Results and Discussion

In the first part of this section, we employed thermal characterization and size exclusion chromatography to assess whether the photoinitiated bulk polymerization of the liquid crystalline thiolene monomers (Table 1) was feasible. A more detailed study of the structure of the obtained polymers was performed using NMR spectroscopy. The remainder of this section will deal with a quantitative analysis of the polymerization of the thiolene monomers.

Thermal Characterization. Monomer samples containing 1% w/w photoinitiator were photopolymerized at various temperatures. Figure 1a shows the DSC heating runs obtained for **ThE 4b4** samples polymerized at 80, 100, and 120, respectively, all after prolonged UV irradiation (>2000 s) in the presence of a photoinitiator.

A melt trajectory is noticeable, starting at approximately 120 °C and ending at approximately 170 °C for the samples polymerized at higher temperatures. The broad melting region can be partly attributed to the molecular weight distribution of the oligomers that is characteristic for step-growth polymerizations. However, from the exothermic signals in the heat flow, we

Scheme 2. Expected ^{13}C NMR-APT Signals of the Aliphatic Region of Poly(ThE 4b4) ("up" for Secondary and Quaternary or "down" for Primary and Tertiary Carbons)[a]

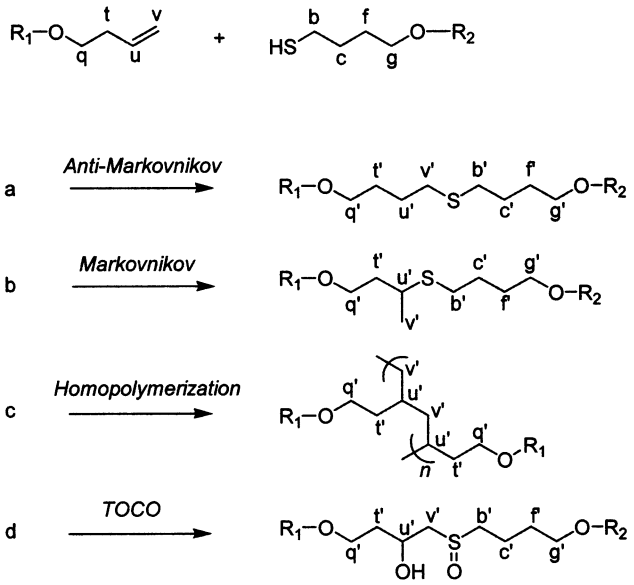

Signal	*a)*	*b)*	*c)*	*d)*
b'	↑	↑	↑	↑
c'	↑	↑	↑	↑
f'	↑	↑	↑	↑
g'	↑	↑	↑	↑
q'	↑	↑	↑	↑
t'	↑	↑	↑	↑
u'	↑	↓	↓	↓
v'	↑	↓	↑	↑

[a] Key: (a) anti-Markovnikov orientation of the thiolene polymer; (b) Markovnikov orientation; (c) homopolymerization of the vinyl group; (d) thiol olefin addition−cooxidation process (TOCO). The NMR signal assignments refer to that of the corresponding monomer.[16]

can conclude that recrystallization effects along with possible crystal−crystal transitions also play an important role. Above 170 °C, the polymers are in the liquid crystalline phase, and the transition to the isotropic phase occurs at approximately 188−190 °C for the samples polymerized at higher temperatures. The shift in both melt transition and clearing point temperatures that occurs upon increasing the polymerization temperature illustrates the effect of higher molecular weights resulting from an increasing conversion with increasing polymerization temperature.

The thermal reactivity of the thiolene monomers and oligomers is illustrated by the first heating curve in Figure 1a for the polymerization at 100 °C, which shows the transitions corresponding to the not-fully converted monomer; the melt transition of the monomer is clearly distinguishable at 55 °C. A reaction exotherm is observed upon heating and the polymerization proceeds to yield a higher molecular weight polymer due to the thermal exposure. Upon cooling and heating once more, the transitions corresponding to a higher molecular weight polymer are recorded (second heating curve in Figure 1a for 100 °C). The cooling runs in Figure 1b demonstrate the reversible character of the mesophase to isotropic transition. Crystallization sets in at approximately 150 °C for the polymerization temperatures

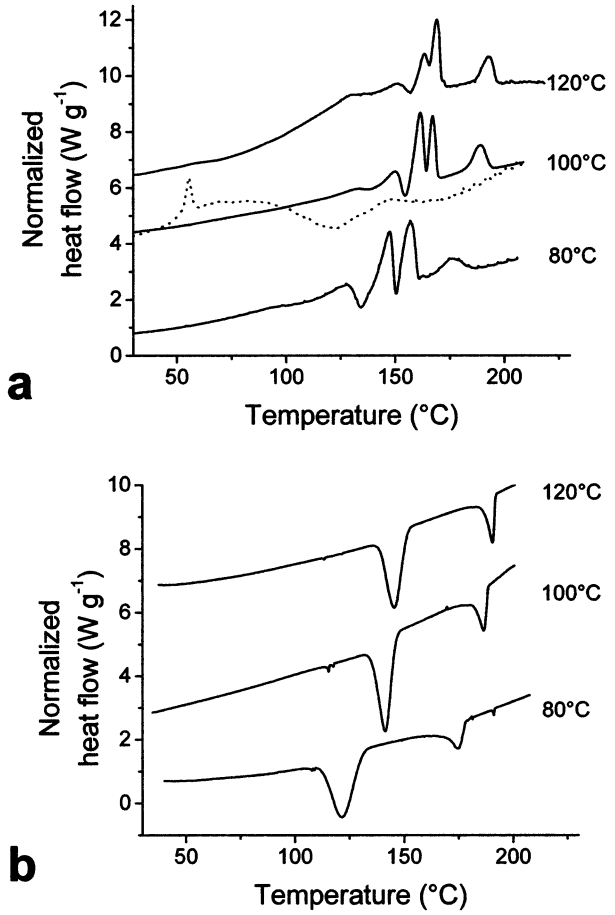

Figure 1. DSC thermograms of **poly(ThE 4b4)** (10 °C min^{-1}), obtained from photoinitiated bulk polymerization at 80, 100, and 120, respectively. The photoinitiator concentration is 1% w/w, based on the monomer. The curves have been shifted vertically for clarity. Key: (a) solid lines, second heating runs; dashed line, first heating run. (b) cooling runs.

Table 2. Transitions (°C) of Poly(ThE *m*b*n*) Homologues[a]

structure	Cr	→	N	→	I
poly(ThE 4b4)		110−175		190−197	
poly(ThE 6b6)		110−155		155−160	

[a] "Cr" denotes the crystalline phase, "N" denotes the nematic phase, and "I" denotes the isotropic phase. The indices *m* and *n* refer to the number of carbon atoms in the spacers.

of 100 and 120 °C, while for 80 °C crystallization sets in at approximately 130 °C.

The transition temperatures could be determined for **poly(ThE 6b6)** in an analogous manner to the results described for **poly(ThE 4b4)** in Figure 1, and its transitions are summarized in Table 2 together with those of **poly(ThE 4b4)**.

The microscope textures reveal a nematic phase texture for all thermotropic liquid crystalline thiolene polymers presented here, as shown in Figure 2 for **poly(ThE 4b4)**, where the characteristic Schlieren texture can be observed. Nematic behavior was also observed for **poly(ThE 6b6)**, where the corresponding monomer also exhibited a smectic A phase next to a nematic phase (shown in Table 1).

Molecular Weight Evaluation. The occurrence of polymerization was confirmed by size exclusion chromatography (SEC). Figure 3 shows the SEC-chromatograms of two **ThE 4b4** samples, polymerized at 150 and 170 °C, respectively. Figure 3a depicts the progress of

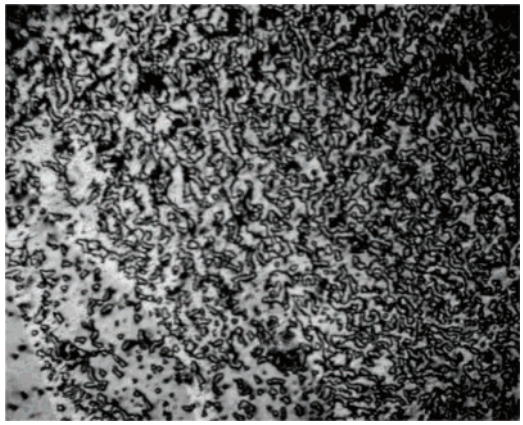

Figure 2. Nematic Schlieren texture of **poly(ThE 4b4)**, viewed between crossed polarizers using optical microscopy.

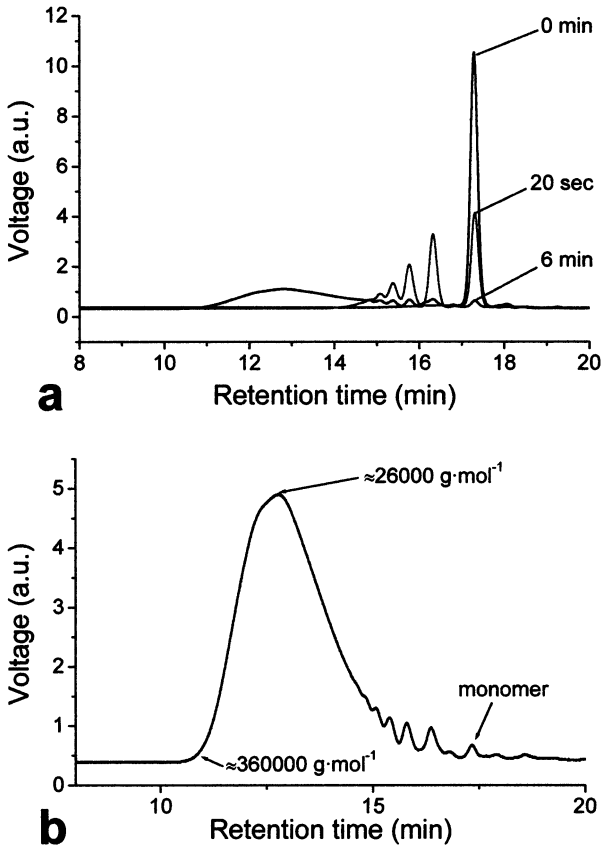

Figure 3. Size exclusion chromatograms of **poly(ThE 4b4)**, obtained upon photoinitiated bulk polymerization (1% w/w photoinitiator): (a) progress of polymerization at 170 °C at the indicated irradiation time; (b) isothermal polymerization at 150 °C for 45 min.

the polymerization reaction at 170 °C at distinct times. The lower oligomeric fractions, e.g., monomer, dimer, and trimer, can be clearly distinguished. Polymerization evidently occurs to a significant degree, taking into account the step-growth polymerization character of thiolene polymerizations. A number-average molecular weight M_n of approximately 26 kg mol^{-1} is obtained for the graph shown in Figure 3b, with a polydispersity M_w/M_n of 2.5, based on polystyrene calibration standards.

Structure Analysis. According to the discussed polymerization mechanism for free-radical propagated thiolene polymerizations, anti-Markovnikov structures are obtained. This statement was checked using ^{13}C

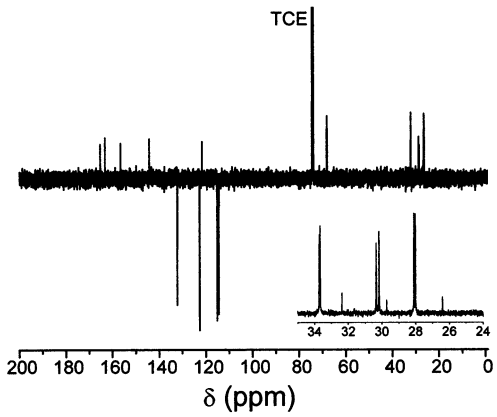

Figure 4. APT-NMR spectrum of **poly(ThE 4b4)** in tetrachloroethane-d_2 (TCE) after photoinitiated isothermal polymerization at 90 °C for 1 h. The inset shows the magnified aliphatic region of a ^{13}C NMR spectrum of the same polymer.

NMR, with the attached proton test (APT), in combination with conventional proton NMR spectroscopy. Using APT, a distinction can be made between secondary and quaternary carbons, both visible as positive signals in the NMR spectrum, and primary and tertiary carbons, visible as negative peaks in the spectrum. Scheme 2 shows the expected signals that can be attributed to thiolenes with anti-Markovnikov and Markovnikov structures. The expected signals corresponding to the polymer structures obtained by homopolymerization and the TOCO-process are also depicted in this scheme.

The dominant signals visible in the APT spectrum of **poly(ThE 4b4)** confirm that the thiolene adducts obtained by photoinitiated polymerization possess the anti-Markovnikov orientation, as shown in Figure 4 (see Experimental Section for a detailed signal assignment).

In comparison to the chemical shifts of the corresponding monomer,[16] the signals of the vinyl group (u, v) are replaced by those of the formed methylene groups u′ and v′ in the polymer (Scheme 2a). The inset in Figure 4 shows an enlargement of the aliphatic region of a ^{13}C NMR spectrum of the same polymer. Additional signals can be identified (along with small signals outside the range shown here at $\delta = 79$, $\delta = 99$, $\delta = 115$, $\delta = 117$, and $\delta = 134$ ppm) that may originate from small fractions displaying Markovnikov orientation (Scheme 2b) or originate from adducts obtained through homopolymerization or partial homopolymerization, or through the TOCO process (Scheme 2c,d). Indications for this are also found in the corresponding proton spectrum where small additional signals can be found at $\delta = 1.35$ (doublet), $\delta = 2.50$, $\delta = 2.75$ and $\delta = 3.00$ ppm, and may be attributed to adducts showing a Markovnikov orientation and/or adducts obtained through the TOCO process. In view of the experimental conditions, where oxygen was not excluded from the surface of the samples, the occurrence of the TOCO process can certainly not be ruled out. Homopolymerization of the vinyl groups was reported to be a negligible side reaction for a similar liquid crystalline diolefin.[13] Homopolymerization of the vinyl moieties in the thiolene monomers described here appears to occur only to a minor degree, based on the almost complete absence of the resonance of the thiol group in the proton NMR spectrum and in the Raman spectrum of the corresponding polymer (see next section).

Although the APT measurement has no quantitative meaning due to the common nuclear Overhauser effect

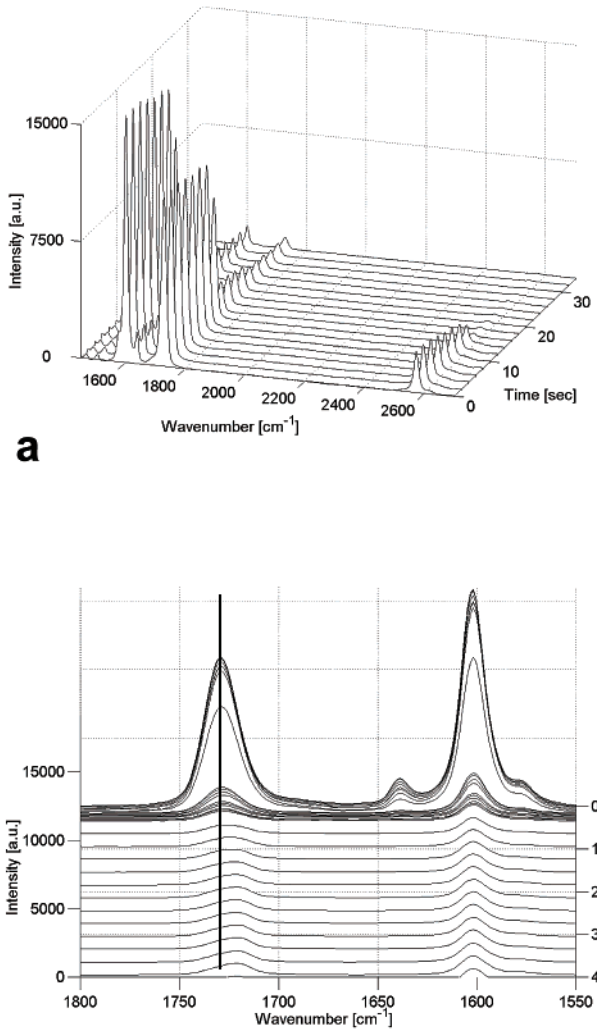

Figure 5. Time-resolved Raman spectra of **poly(ThE 4b4)**, obtained upon photoinitiated isothermal polymerization at 150 °C (1% w/w photoinitiator): (a) spectral range from 1500 to 2700 cm^{-1}; (b) magnification of the carbonyl band (1729 cm^{-1}) area. The vertical line through the peak maximum serves to illustrate the gradual shift of the carbonyl peak position.

and the different relaxation times for dissimilar substituted carbons, the fraction of polymers exhibiting configurations different from the expected anti-Markovnikov orientations can be estimated to be less than 5% based on the proton NMR spectra.

Time-Resolved Raman Spectroscopy. A quantitative analysis of the monomer conversion was performed for in situ photopolymerized thiolene monomers at different temperatures using time-resolved Raman spectroscopy. Raman spectroscopy is preferred over FTIR spectroscopy as the intensity of the thiol band is stronger in Raman spectroscopy, due to the strong polarizability of the thiol group. Figure 5a shows the time-resolved Raman spectra for in situ photopolymerized **ThE 4b4** at 150 °C, in the spectral range from 1500−2700 cm^{-1}, which is representative for plots obtained at other temperatures. The Raman shifts characteristic for the aromatic ring vibration (1602 cm^{-1}), the vinyl group (1641 cm^{-1}), the carbonyl group (1729 cm^{-1}), and the thiol group (2573 cm^{-1}) can be distinguished.

An absolute decrease of the spectral bands of both reactive groups is visible, confirming the polymerization of the monomer. The conversion can be monitored as a function of time by comparison of the ratio of either the vinyl or thiol group to an internal standard, such as the carbonyl band or the band of the aromatic ring vibration. Equation 1 shows this calculation for the partial conversion of the thiol group and the vinyl group, neglecting end group contributions:

$$p^t_{SH} = 1 - \left(\frac{I^t_{SH}/I^t_{Rf}}{I^0_{SH}/I^0_{Rf}}\right) \qquad p^t_{C=C} = 1 - \left(\frac{I^t_{C=C}/I^t_{Rf}}{I^0_{C=C}/I^0_{Rf}}\right) \quad (1)$$

where p^t_{SH} and $p^t_{C=C}$ are the partial conversions of the thiol and vinyl group, respectively, I^t_{SH} and $I^t_{C=C}$ are the peak intensities or peak areas of the thiol and vinyl spectral bands, and I^t_{Rf} refers to the spectral band of an internal standard, all at time t during polymerization. This ratio is compared to the initial ratio before polymerization of both spectral bands, at time $t = 0$ s.

The overall intensity of the spectral bands drops relatively quickly (on the order of 10 s) after the polymerization is initiated, similar to observations made in FTIR studies.[26,27] This effect results from phase separation of the oligomeric/polymeric species from the initially isotropic monomeric liquid. The intensity of the backscattered Raman radiation that is collected on the spectrometer will depend on the balance between two factors:[28] (a) the sample volume exposed by the incident light, which would be less for a diffusely scattering, phase-separated sample, and (b) the number of Raman events per unit volume, which would be more in a scattering, phase-separated sample. In our case, it appears that factor a, i.e., the volume exposed to the incident light, predominates.

Phase separation is observed for all samples polymerized at the investigated temperatures but the onset of phase separation is shifted to longer times with increasing polymerization temperature (a shift of approximately 7 s at 90 °C to about 15 s at 150 °C). Whereas there is no shift of all peak positions over time, the carbonyl band starts at 1729 cm^{-1} and, as the polymerization progresses, gradually shifts to 1720 cm^{-1} immediately after phase separation sets in (Figure 5b). This indicates that the environment of the carbonyl group changes immediately upon phase separation due to the formation of oligomeric species. The introduced heterogeneity is reflected by the shift of the carbonyl band from its original position.

Although the carbonyl band can in principle function as the internal standard, the aromatic ring vibration band at 1602 cm^{-1} was taken as the internal standard, since the more asymmetric carbonyl band is more susceptible to changes in the carbonyl group environment. Figure 6a shows the conversion of both the vinyl and the thiol group as a function of time for several polymerization temperatures.

The time-resolved Raman experiments show that high overall conversions are obtained in a short period of time (e.g., >70−80% after 10−90 s). The reaction rate increases with increasing temperature, as can be deduced from the slope of the curves at the early stages of the reaction. The scattering in the data results from the decreased signal-to-noise ratio immediately after phase separation sets in. In addition, as the reaction progresses, the baseline of the spectra rises due to fluorescence effects, especially around the thiol peak position.

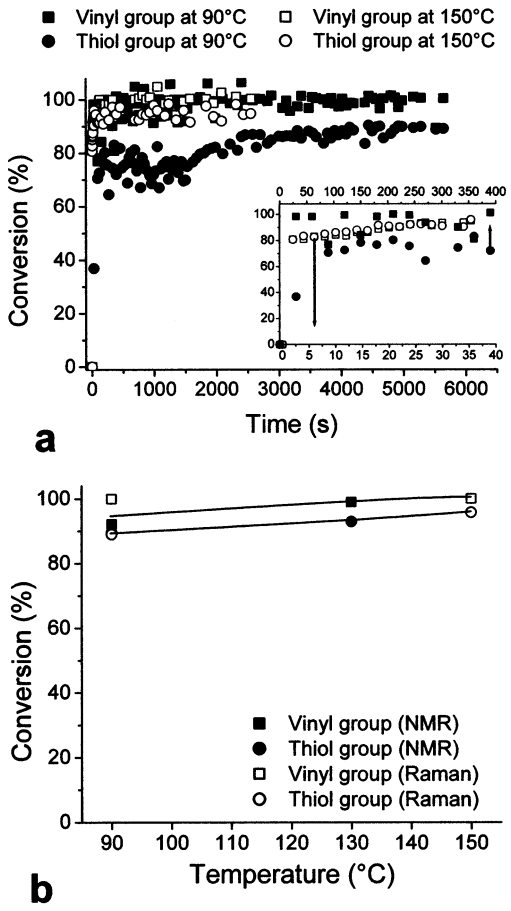

Figure 6. Conversion plots of isothermally photopolymerized **ThE 4b4**, containing 1% w/w photoinitiator, at the indicated temperatures. (a) Conversions of the thiol and vinyl group as a function of time, using time-resolved Raman spectroscopy. The inset shows an enlargement of the initial stage of the polymerization (90 °C, top time axis; 150 °C, bottom time axis). (b) Ultimate conversions of the thiol and vinyl group as a function of the isothermal polymerization temperature, determined using time-resolved Raman spectroscopy and ^{1}H NMR spectroscopy.

When a differentiation is made between the conversions of both reactive groups, it is noted that the partial conversion of the vinyl group exceeds that of the thiol group. The higher consumption of the vinyl group in comparison to the thiol group could be the result of side reactions such as the formation of carbon−carbon bonds due to homopolymerization of the vinyl group, as suggested in the literature.[29] This would explain the lower ultimate partial thiol conversion. This effect is more prevalent at a lower polymerization temperature, suggesting that the ratio between thiolene addition and homopolymerization of the vinyl bond shifts in favor of the thiolene reaction at higher temperatures. On the other hand, the higher thiol consumption at higher temperatures could also be attributed to side reactions involving the thiol moiety, such as disulfide formation or a transesterification reaction where the thiol group reacts with the aromatic ester moiety to yield a thioester adduct.[13] This may explain why the conversion of the thiol group approaches that of the vinyl group. The difference in partial conversion of the thiol and vinyl groups is confirmed by an earlier study involving a triple

phenyl ring thiolene.[30] It was found that the overall conversion increased if the thiol−olefin stoichiometry was adjusted in favor of the vinyl group to compensate for the higher vinyl consumption.

The ultimate conversion increases with increasing polymerization temperature for the investigated temperature range, and approaches almost complete conversion of the vinyl bonds at higher temperatures, based on both time-resolved Raman spectroscopy measurements and proton NMR spectroscopy (Figure 6b). The term "ultimate" conversion should be used with care since post-polymerization processes are not uncommon in free-radical-based polymerizations, once the irradiation is stopped.[31] However, from the conversion curves (Figure 6a), it seems justified to speak of an ultimate conversion in view of the long polymerization times and the plateau values that were reached for the conversions. The higher values for the ultimate conversion at higher temperatures suggest an effect of crystallization during the course of the polymerization process. Crystallization reduces the monomer mobility and retards the polymerization, leading to a lower overall conversion. This is supported by the earlier mentioned delay in the onset of crystallization, when the temperature is raised and the polymerization temperature approaches the crystallization temperature of the polymer (Figure 1b). The driving force for crystallization is lower and crystallization is delayed, thus enabling a higher overall conversion at higher polymerization temperatures. Although the influence is not detected here, a ceiling temperature effect may start to play a more pronounced role above the crystallization temperature of the polymer. From that point on, the contribution from the crystallization process to the free energy change for the propagation process is diminished, thus making the free energy change less negative, similar to the situation encountered for addition polymerizations.[32,33] A further increase in temperature could then be reflected in a lower molecular weight of the polymer as the reverse reaction in the usually rate-determining step (Scheme 1, part III) becomes more significant.

Conclusions

Liquid crystalline thiolene monomers based on a phenyl benzoate core can be polymerized substantially in bulk, and the polymerization can be initiated on demand by UV-irradiation. The liquid crystalline thiolene polymers exhibit a nematic mesophase, and the molecular weight and molecular weight distribution are typical for polymers obtained by a step-growth polymerization. Anti-Markovnikov structures are predominantly formed, with a small fraction of the structures displaying different configurations that can be attributed to thiol olefin addition−cooxidation processes or to homopolymerization of the olefinic moiety. The partial conversions of the thiol and vinyl groups were readily monitored using time-resolved Raman spectroscopy and dissimilar partial reaction rates were demonstrated. An optimal effective stoichiometry, and hence an optimal overall conversion, can be achieved by adjusting the initial thiol−olefin ratio to compensate for a higher consumption of one of the groups.

References and Notes

(1) Broer, D. J.; Van Haaren, J. A. M. M.; Van de Witte, P.; Bastiaansen, C. *Macromol. Symp.* **2000**, *154*, 1−13.

(2) Friend, R. H.; Gymer, R. W.; Holmes, A. B.; Burroughes, J. H.; Marks, R. N.; Taliani, C.; Bradley, D. D. C.; Dos Santos, D. A.; Brédas, J. L.; Lögdlund, M.; Salaneck, W. R. *Nature (London)* **1999**, *397*, 121−128.

(3) Jagt, H.; Dirix, Y.; Hikmet, R.; Bastiaansen, C. *Adv. Mater.* **1998**, *10*, 934−938.

(4) Van Duijnhoven, F. G. H.; Bastiaansen, C. W. M. *Appl. Opt.* **1999**, *38*, 1008−1014.

(5) Collyer, A. A. *Liquid Crystal Polymers: From Structures to Applications*; Elsevier Applied Science: London, 1992.

(6) Mori, H.; Itoh, Y.; Nishiura, Y.; Nakamura, T.; Shinagawa, Y. *Jpn. J. Appl. Phys., Part 1* **1997**, *36*, 143−147.

(7) Broer, D. J.; Boven, J.; Mol, G. N. *Makromol. Chem.* **1989**, *190*, 2255−2268.

(8) Broer, D. J.; Lub, J.; Mol, G. N. *Macromolecules* **1993**, *26*, 1244−1247.

(9) Hikmet, R. A. M.; Lub, J.; Higgins, J. A. *Polymer* **1993**, *34*, 1736−1740.

(10) Crawford, G. P.; Zumer, S. *Liquid Crystals in Complex Geometries. Formed by Polymer and Porous Networks*; Taylor & Francis: London, 1996.

(11) Drzaic, P. S. *Liquid Crystal Dispersions*; World Scientific: Singapore, 1995.

(12) Jacobine, A. F. In *Radiation Curing in Polymer Science and Technology*; Fouassier, J. P., Rabek, J. F., Eds.; Elsevier Applied Science: London, 1993; Vol. 3, Chapter 7.

(13) Lub, J.; Broer, D. J.; Van den Broek, N. *Liebigs Ann./Recl.* **1997**, 2281−2288.

(14) Lub, J.; Broer, D. J.; Martinez Antonio, M. E.; Mol, G. N. *Liq. Cryst.* **1997**, *24*, 375−379.

(15) Lub, J.; Broer, D. J.; Allan, J. F. *Mol. Cryst. Liq. Cryst.* **1999**, *332*, 259−266.

(16) Wilderbeek, H. T. A.; Van der Meer, M. G. M.; Jansen, M. A. G.; Nelissen, L.; Fischer, H. R.; Van Es, J. J. G. S.; Bastiaansen, C. W. M.; Lub, J.; Broer, D. J. *Liq. Cryst.* **2002**, in press.

(17) Wilderbeek, H. T. A.; Van der Meer, M. G. M.; Bastiaansen, C. W. M.; Broer, D. J. *J. Phys. Chem. B.* **2002**, in press.

(18) Fouassier, J. P. In *Radiation Curing in Polymer Science and Technology*; Fouassier, J. P., Rabek, J. F., Eds.; Elsevier Applied Science: London, 1993; Vol. 2, Chapter 1.

(19) Hoshino, M.; Shizuka, H. In *Radiation Curing in Polymer Science and Technology*; Fouassier, J. P., Rabek, J. F., Eds.; Elsevier Applied Science: London, 1993; Vol. 2, Chapter 15.

(20) Walling, C.; Helmreich, W. *J. Am. Chem. Soc.* **1958**, *81*, 1144−1148.

(21) Markovnikov's rule states that the proton is added to the carbon atom already bearing the most protons. For an anti-Markovnikov adduct, the opposite is true.

(22) Kharasch, M. S.; Nudenberg, W.; Mantell, G. J. *J. Org. Chem.* **1951**, *16*, 524−532.

(23) Szmant, H. H.; Mata, A. J.; Namis, A. J.; Panthananickal, A. M. *Tetrahedron* **1976**, *32*, 2665−2680.

(24) D'Souza, V. T.; Vaidyanah, K. I.; Szmant, H. H. *J. Org. Chem.* **1987**, *52*, 1725−1728.

(25) Wilderbeek, H. Ph.D. Thesis, Eindhoven University of Technology, Eindhoven, The Netherlands, 2001; ISBN 90-386-2972-9.

(26) Bhargava, R.; Wang, S.-Q.; Koenig, J. L. *Appl. Spectrosc.* **1998**, *52*, 323−328.

(27) Bhargava, R.; Wang, S.-Q.; Koenig, J. L. *Macromolecules* **1999**, *32*, 8989−8995.

(28) Rastogi, S.; Goossens, J. G. P.; Lemstra, P. J. *Macromolecules* **1998**, *31*, 2983−2998.

(29) Nuyken, O.; Hofinger, M. *Polym. Bull. (Berlin)* **1981**, *4*, 75−82.

(30) Van den Broek, N. Master Thesis, Eindhoven University of Technology, Eindhoven, The Netherlands, 1994.

(31) Kloosterboer, J. G. *Adv. Polym. Sci.* **1988**, *84*, 1−61.

(32) Sawada, H. In *Thermodynamics of Polymerisation*; O'Driscoll, K. F., Ed.; Marcel Dekker Inc.: New York, 1976; Chapter 1.

(33) Ivin, K. J. *J. Polym. Sci., Part A: Polym. Chem.* **2000**, *38*, 2137−2146.

MA020916L